PAPER • **OPEN ACCESS**

Performance improvement of a Vestas V52 850kW wind turbine by retrofitting passive flow control devices

Journal of Physics: Conference Series **2767** (2024) 022027 doi:10.1088/1742-6596/2767/2/022027

Performance improvement of a Vestas V52 850kW wind turbine by retrofitting passive flow control devices

M Manolesos[a,b,g], Y Celik[a,f], H Ramsay[a,b], R Karande[c], B Wood[c], I Dinwoodie[g], I Masters[a], M Harrold[e], G Papadakis[g]

[a] Swansea University, UK
[b] City, University of London, UK
[c] Anakata Wind Power Resources, UK
[d] Natural Power, UK
[e] Offshore Renewable Energy Catapult, UK
[f] Hakkari University, Turkey
[g] National Technical University of Athens, Greece

marinos@fluid.mech.ntua.gr

Abstract. This study presents the results of a collaborative effort between academia and industry aimed at further enhancing the benefits provided by Vortex Generators and Gurney Flaps. To achieve this objective, an integrated approach was employed, involving wind tunnel experiments, on-site measurements, and computational simulations to design devices tailored for an onshore (Vestas V52, 850 kW) turbine and assess their influence on turbine performance. Device selection was based on wind tunnel measurements, while their positioning on the blade was based on infrared thermography images from the field. A Reynolds Averaged Navier Stokes solver was used to predict the performance of the devices on both airfoil and blade level. The final assessment of the upgrade pack was based on SCADA data and Lidar measurements. The results show that an Annual Energy Production uplift of 5.77% is measured for this turbine.

1. Introduction

Among the passive flow control devices used to improve wind turbine performance, Vortex Generators (VGs) and Gurney Flaps (GFs) are an attractive combination [1–4]. VGs generate streamwise vortices, which energise the boundary layer over airfoils and blades. GFs change the Kutta condition at the trailing edge of an airfoil or blade, increasing lift and drag for a given angle of attack.

In the case of wind turbines, both devices are used to improve the performance of the rotor, making them an inexpensive means of increasing energy yield. Vane VGs are used at the root region of the blade (inboard) to suppress flow separation and at the tip region to counteract the negative effects of roughness [5–8]. The expected gain is approximately 2-3% in Annual Energy Production (AEP) [1].

A range of experimental and numerical studies on vortex generators (VGs) have been conducted [9–12], providing insights into flow mechanisms and design approaches. Several parameters are crucial in the downstream evolution of streamwise vortices caused by VGs, influencing aerodynamic performance, such as VG height, distance, orientation, angle to the oncoming flow and chordwise location [7,13]. Vane type VGs remain the industry standard despite some studies indicating that aerodynamically shaped VGs show promise [14–16].

Tian et al.[17] found that VGs can improve turbine performance by suppressing flow separation and mitigating soiling effects. Zhao et al.[18] further investigated the impact of transition on blade

performance, with VGs shown to be effective in promoting performance in the inner part of the blade. Mueller-Vahl et al.[19] focused on optimizing VGs, identifying the optimal chordwise position and spanwise spacing to achieve a smooth post-stall lift curve. Wu et al.[20] investigated the effect of the VGs at the transitional area of a 1.5 MW wind turbine blade. One of the main findings obtained from their study was that VGs changed the aerodynamic performance at the transition area of the blade, improving torque and restraining flow separation. Overall, it is generally accepted that retrofitted VGs can enhance wind turbine performance.

Gurney Flaps (GFs) are quite common in the motorsport industry but have recently shown promising results for wind turbine applications [21]. In general, they should be small (25% of the boundary layer height at the trailing edge) in order to achieve an increase in Lift to Drag ratio [3].

To date, no research study has covered the complete route from passive flow control device design to installation on the field and assessment, which is the aim of the present study. The findings of a collaborative effort between academia and industry are presented, where enhanced VGs and GFs were designed, installed and assessed. To achieve this goal, an integrated approach was employed, including wind tunnel testing, Computational Fluid Dynamics (CFD) simulations and field measurements, and an onshore (Vestas V52, 850kW) turbine was considered. More specifically, wind tunnel tests were performed at Swansea University (SU). CFD simulations were performed by SU, the National Technical University of Athens (NTUA) and Anakata Wind Power Resources (Anakata), while BEM predictions were provided by Anakata. Flow control device designs were provided by SU and Anakata, while Anakata also proposed device locations on the turbine blade in collaboration with NTUA. Natural Power performed a comparative performance assessment of the upgrade pack effect on the turbine performance. Offshore Renewable Energy Catapult coordinated and partly funded the project.

The paper is structured as follows. First the methodology is described in Section 2, discussing experimental, numerical, and field measurement tools. Section 3 presents the results, focusing on the device selection process, device positioning, numerical predictions, and final assessment, while Section 4 concludes the paper.

2. Methodology

2.1. Experimental setup

Swansea University low speed wind tunnel (see Figure 1) was used for the experiments, which included pressure and time-resolved measurements, tuft flow visualizations and Infrared (IR) Thermography on 18% thick NACA63(3)-618 airfoil. The wind tunnel section has 1.5 m in width and 1 m in height, with a maximum speed of 50 m/s. The free stream turbulence intensity is 0.3%. Boundary layer transition was controlled using a 0.4mm high 60° zigzag tape. All tests were performed at Re = 1.5M.

2.2. CFD Approach

In this section the employed solver, the way to model the VG effect and the validation of the numerical approach against independently published data is presented for an airfoil profile and the V52 blade.

2.2.1. Solver

The flow characteristics and aerodynamic performance of airfoils and the turbine blade with and without VGs have been investigated by numerically solving the Unsteady Reynolds-Averaged Navier Stokes (URANS) equations with an in-house solver, MaPFlow [22], which can handle both compressible and fully incompressible flows on arbitrary polyhedral meshes by employing a cell-centred finite volume discretization process. In each of the cases presented here, the flow was considered fully incompressible, and the k-ω SST turbulence model was employed. The GFs were not considered in the simulations.

2.2.2. Vortex Generator modelling

Fully resolving the VG geometry on the airfoils and blades was not considered in this study due to the prohibitive computational cost. Instead the popular BAY model in its jBAY version was employed [23]

following the guidelines presented in [24]. This approach has been extensively validated in MaPFlow for airfoils and wind and tidal turbine applications [11,24–26] .

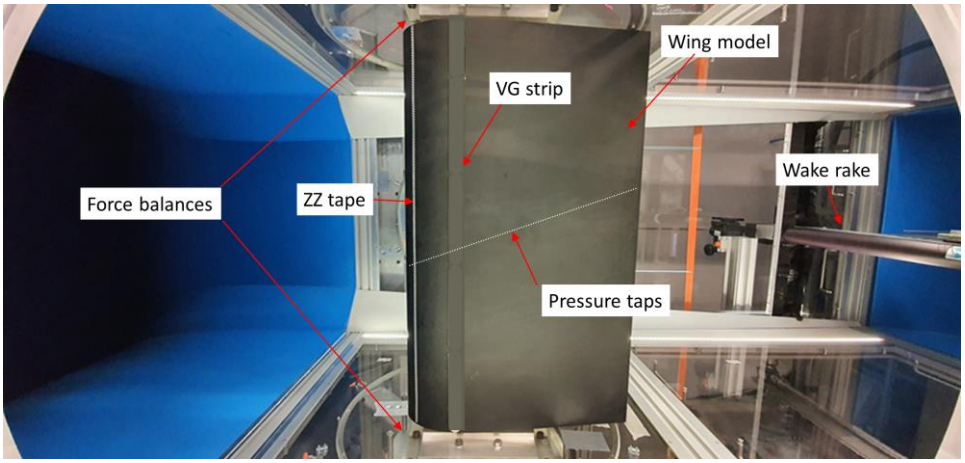

Figure 1. Sideview of the set up at Swansea University wind tunnel

2.2.3. NACA63(3)-618 airfoil modelling

An O-type hybrid mesh, which consisted of both structured and unstructured domains, was used for the 2D airfoil simulations. The far-field was located at a distance of 50 c, as a compromise between computational time and accuracy [27]. The boundary layer mesh had 50 layers with a first cell height of 1.45×10^{-5}m to achieve $y^+ < 1$ throughout the airfoil surface. The Reynolds number was 1.5×10^6 to match the number tested in wind tunnel tests. The mesh and selected details are shown in Figure 2.

Five different total number of nodes on the airfoil were examined, namely 400, 800, 1200, 1800, and 2400, at two different angles of attack. Figure 3 (left) shows the comparison of lift coefficients as a function of the number of airfoil surface nodes. It is evident that there were no significant changes in the lift coefficient for the investigated angles of attacks when the number of nodes exceeded 1200. Consequently, 1200 nodes were chosen for subsequent analyses, resulting in a final 2D mesh comprising approximately 97,000 mesh cells.

The selected 2D mesh was extruded in the spanwise direction to create a low-aspect-ratio CFD domain (here named the 3D-slice domain) for the aerodynamic analysis of the airfoil equipped with a VG pair. The main purpose of using the 3D-slice domain for the performance analysis of the VGs is to strike a balance between computational cost and accuracy [11]. Figure 4 shows the extruded airfoil with a single pair of VGs located on the suction side. A symmetry boundary condition was used at the sidewalls of the computational domain (which are not shown in Figure 4 for clarity). The total number of cells in the extruded CFD domain was approximately 9 million.

Figure 3 (right) presents a comparison of the lift coefficients obtained using the current 2D CFD, current 3D-Slice CFD, and experimental data [21], plotted against the angle of attack. The figure shows that while the CFD predictions closely match the experimental measurements at low angles of attack, discrepancies increase at higher angles, as expected [25]. Additionally, the lift coefficients obtained from the 2D CFD model and the 3D-Slice CFD model without VGs yield similar results, suggesting that the 3D-Slice airfoil has low aspect ratio limiting its ability to generate sufficient 3D flows over the airfoil.

2.2.4. V52 turbine blade modelling

For the turbine simulations, a single blade was modelled using a rotational periodic boundary condition. The moving reference frame model was also employed to account for rotational effects within the rotating zone. Using the location of the wind turbine as the reference point, the distance to the upstream boundary is approximately 10 times the rotor radius (10R), while the distance to the downstream

boundary is around 20 times the rotor radius (20R). The operating conditions for the turbine model were obtained through SCADA data from the V52 test turbine.

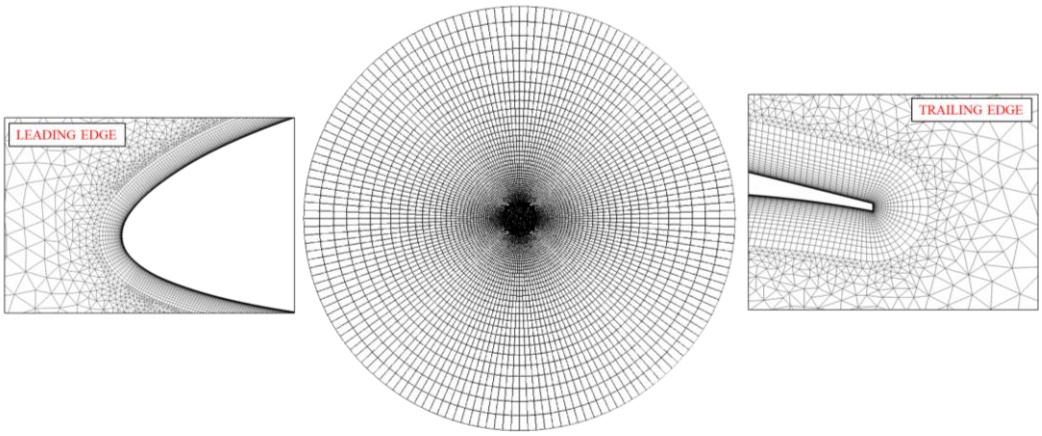

Figure 2. *Airfoil mesh details*.

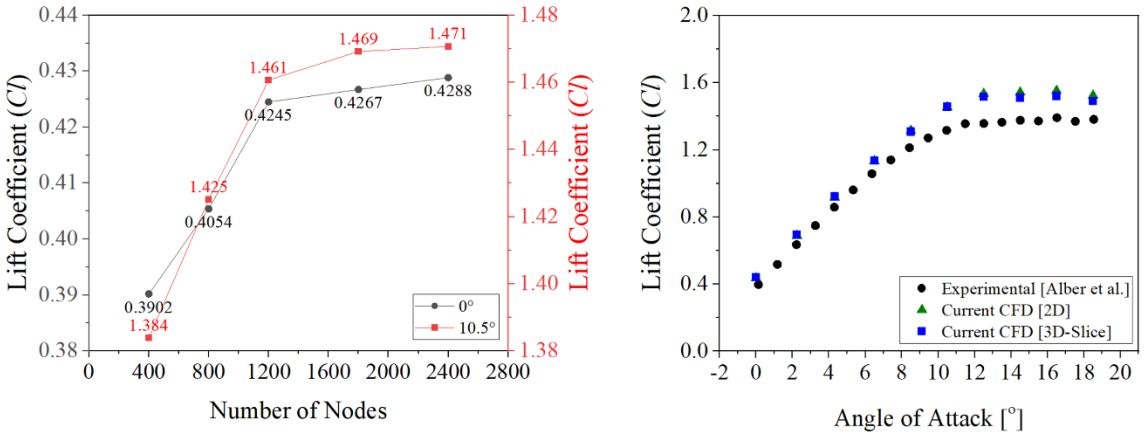

Figure 3. (left) Lift coefficient versus number of nodes on the airfoil for α=0° and α=10.5°; (right) Comparison of CFD predicted lift coefficient with experimental data [21].

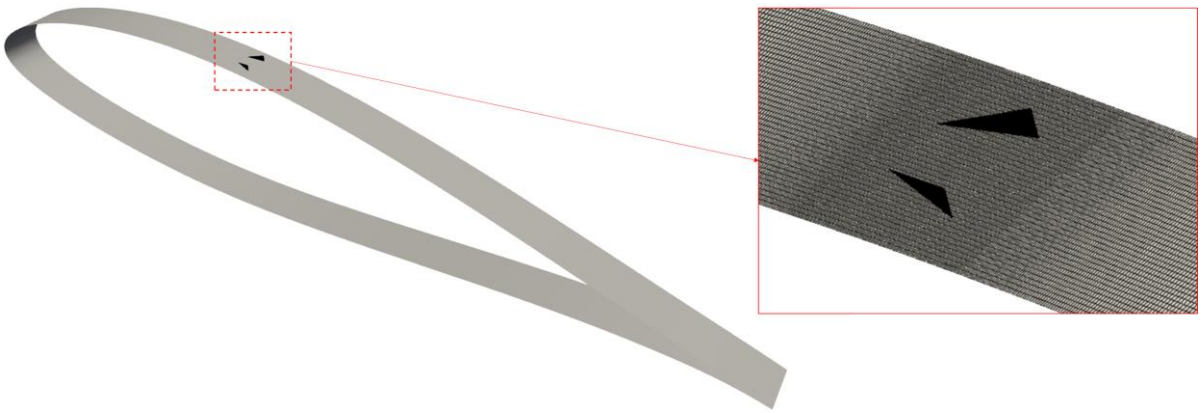

Figure 4. Mesh demonstration over the extruded NACA63(3)-618 airfoil with one VG pair on the suction side.

The computational grid generated for the V52 turbine blade was a structured grid with denser meshes applied to the inboard and outboard regions of the blade where the VGs were placed. To maintain a y^+ value of approximately 1 for all simulations, the first cell thickness of the boundary layer mesh layer was set to 1.75×10^{-6} with 60 inflation layers. It is noted that, as shown in Figure 5, left, the mesh at the locations of the VGs was significantly denser to properly model their effect. Consequently, the total number of cells was approximately 66 million.

To validate the numerical approach, the CFD results of the turbine blade without VGs are compared with publicly available field data [28] for the power output as a function of various wind speeds, as illustrated in Figure 5, right. As seen in the figure, the power output curve obtained with the current CFD model is in good agreement with the field test results for nearly all investigated wind speeds. It is also important to note that to ensure consistency between the results, the mesh with the denser region has been used for the simulations with and without the VGs.

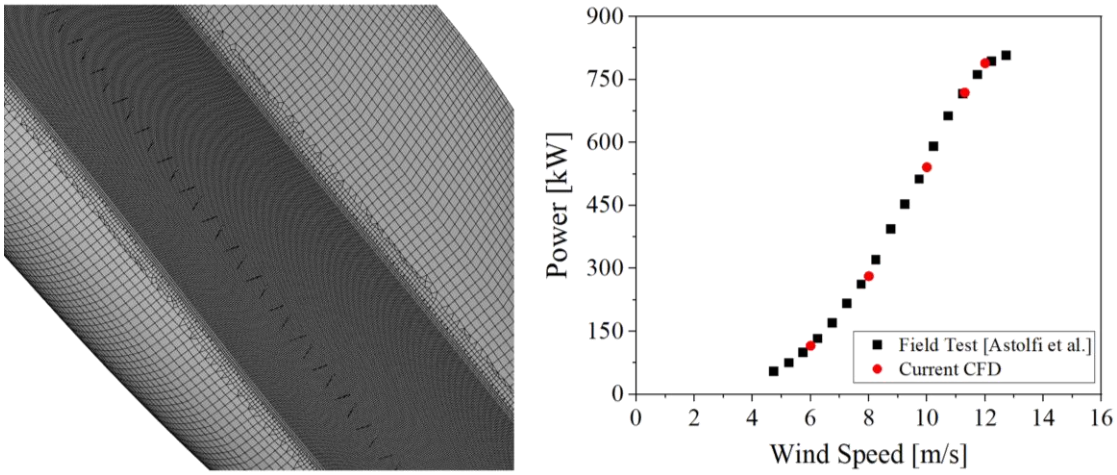

Figure 5. (left) Detail of the V52 blade mesh close to the root region where VGs were installed. (right) Comparison of the power output obtained from current CFD model without VGs with field test data [28].

2.3. Field measurements

2.3.1. Infrared *Thermography*

Infrared thermography was used to examine the blade leading edge surface condition, to identify the extent of the separated flow in the root region and to further validate the blade resolved simulations. A ground based custom system developed by Anakata was used to record videos downstream of the rotor.

2.3.2. Lidar Measurements

A nacelle mounted Epsiline WindEagle Lidar with a wind angle ±60°, an operating range 0.5 - 27 m/s and an accuracy of 0.1m/s was used in addition to the turbine anemometer for wind speed velocity measurements. The Lidar data were acquired for a total of five months.

3. Results

3.1. Passive flow control device selection

During the wind tunnel tests, over 100 different individual VG configurations were tested, including a parametric study on vane-type VGs and various versions of 3D-shaped VGs. The latter encompassed a wide range of aerodynamically shaped VGs, such as strake-type, bargeboard-type, and airfoil-type, single as well as double row VGs. It is out of scope for this paper to present the complete set of results and the findings of the extensive parametric study, hence only the best performing VGs are presented, see Figure 7 (left). All non-standard vane type designs were provided by Anakata.

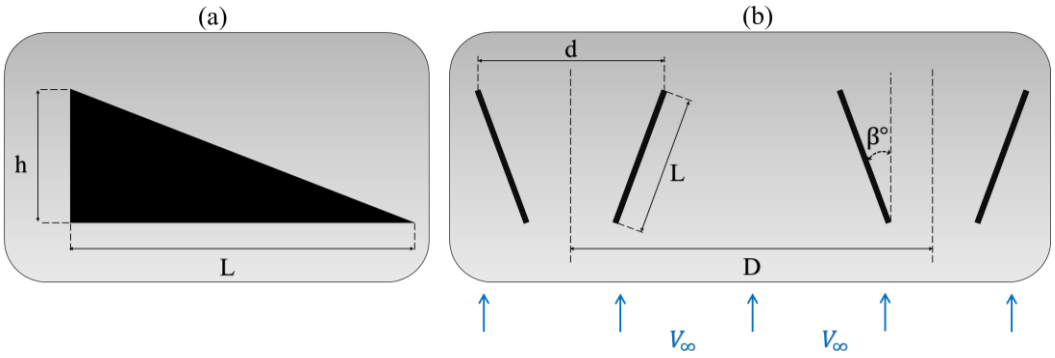

Figure 6. Vane type VG parameters. (a) Side view; (b) Top view.

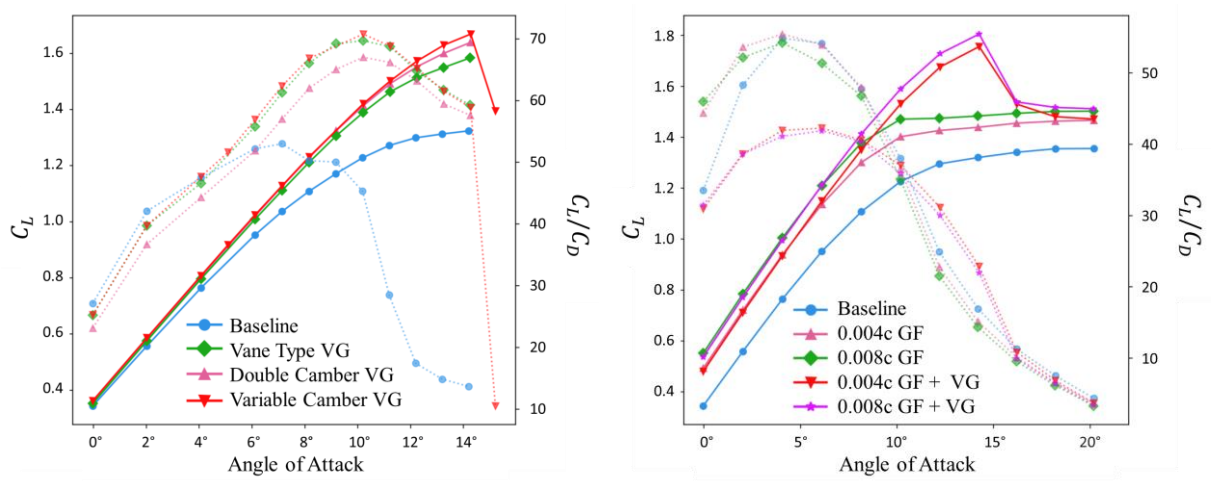

Figure 7. Lift coefficient and lift to drag ratio performance of the three best performing VGs (left) and the two most promising GFs (right). Wind tunnel measurements.

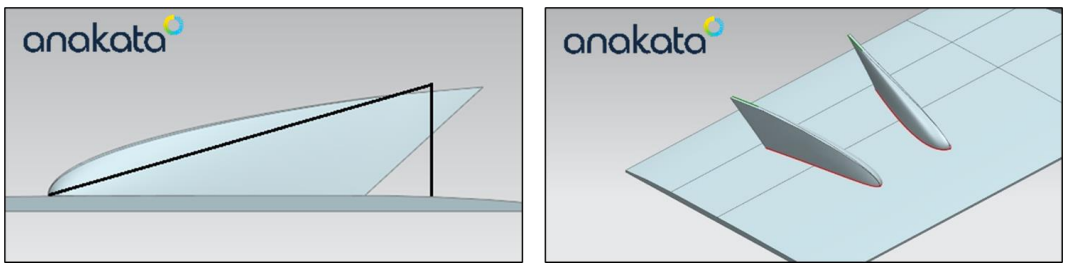

Figure 8. The aerodynamically shaped VG selected for application on the V52 blade in side and 3D view.

The best performing VG (Figure 8) was a 3D, aerodynamically shaped VG with varying camber and had the same VG pair distance and VG distance as the best performing vane VG configuration, but was 0.003c higher (see Figure 6 and Table 1). The 3D shaped VG provided higher lift at higher angles of attack for the same L/D performance and was selected for installation on the V52 blades.

A number of traditional and serrated GFs were tested in the wind tunnel and the performance of the most promising ones are shown in Figure 7 (right), also in combination with VGs. The 0.004c high GF was selected for installation on the V52 blades.

Table 1. Design parameters of selected Vortex Generator and best performing Vane Vortex Generator

Vane / 3D shaped?	VG angle, β	VG height, h/c	VG pair distance, D/h	VG distance, d/h	VG Aspect Ratio, L/h	Chordwise location, x/c
3D Shaped	15°	1.0%	7	3.5	3	40%
Vane	15°	0.7%	7	3.5	3	40%

3.2. Passive flow control device positioning on the blade

Figure 9 shows an IR image of the complete blade, highlighting the natural transition line, early transition due to leading edge erosion and the 3D separated flow region close to the root. Figure 10 (left) shows a comparison of the CFD surface streamlines with the IR image for the uncontrolled case, close to the root. The 3D separated flow region is captured very well by the simulations. The VG positions on the blade were decided based on both infrared measurements and CFD simulations. In total VGs covered approximately 19% and 36% of the blade radius close to the root and tip, respectively.

The GF location was based on additional wind tunnel data for a 35% thick airfoil, not presented here, and a blade resolved CFD and BEM sensitivity analysis. The GF extended for ~31% of the blade radius close to the root region.

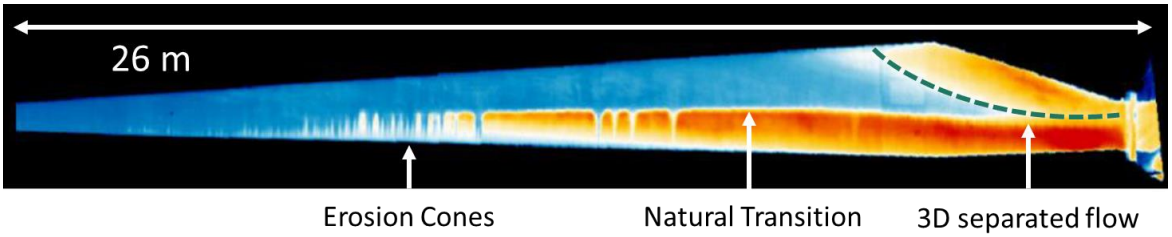

Figure 9. Anakata infrared thermography image from the suction side of V52 turbine blade without Vortex Generators.

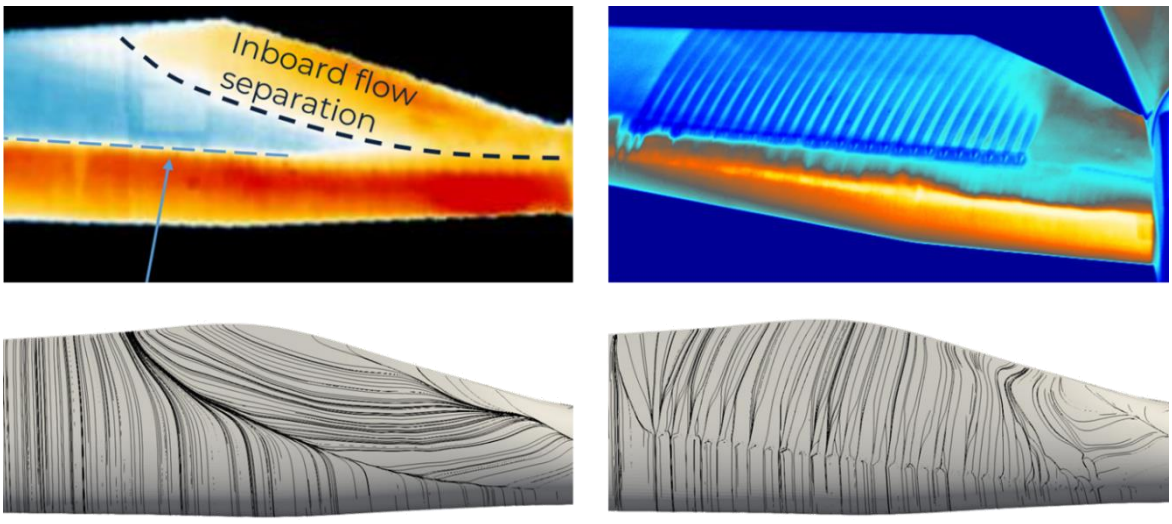

Figure 10. Comparison of CFD streamlines and infrared thermography images at the root region of the V52 wind turbine blade at 8 m/s wind speed with (right) and without (left) Vortex Generators.

3.3. Vortex Generator performance modelling

As detailed in section 2.2.3, the 3D-slice simulations overpredict the baseline airfoil performance at high angles of attack. As a result, a direct agreement between the wind tunnel measurements and the CFD

predictions is not expected. However, the trends were captured successfully by the 3D-slice simulations and the relevant performance improvement was accurately predicted, see Figure 11.

The blade simulations with and without the VGs were in good agreement with the IR field measurements, see Figure 10. In terms of performance, CFD predicted 1.1% and 5.5% increase in power at 8m/s windspeed, when only the inboard (root) or both inboard and outboard (tip) VGs were employed, see Figure 12, left. Based on these results and the site wind distribution the predicted AEP uplift for installing both inboard and outboard VGs is 4.3%.

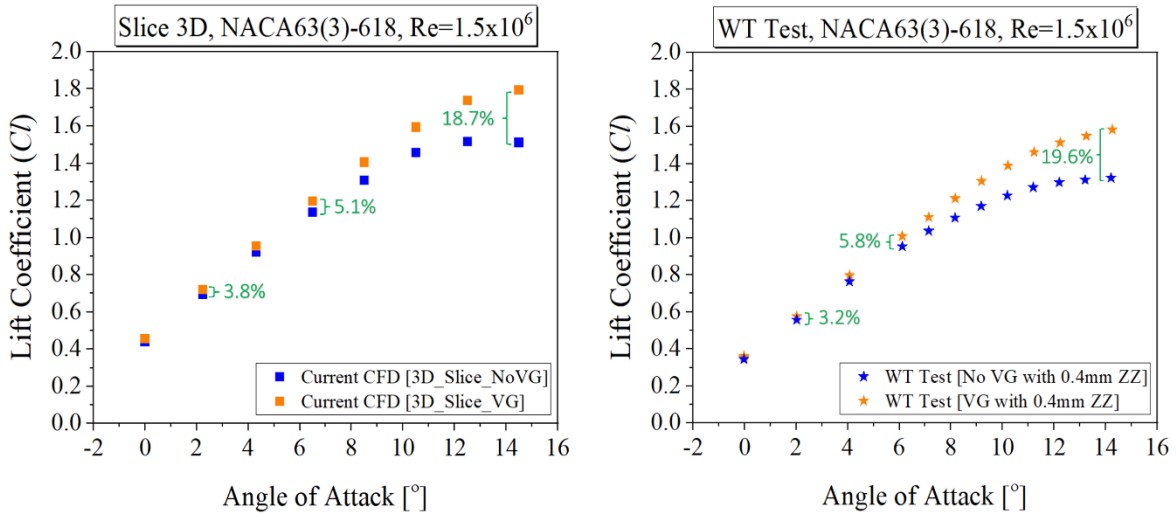

Figure 11. Performance comparison of the VGs located on the suction side of the NACA63(3)-618 airfoil from CFD and wind tunnel investigations.

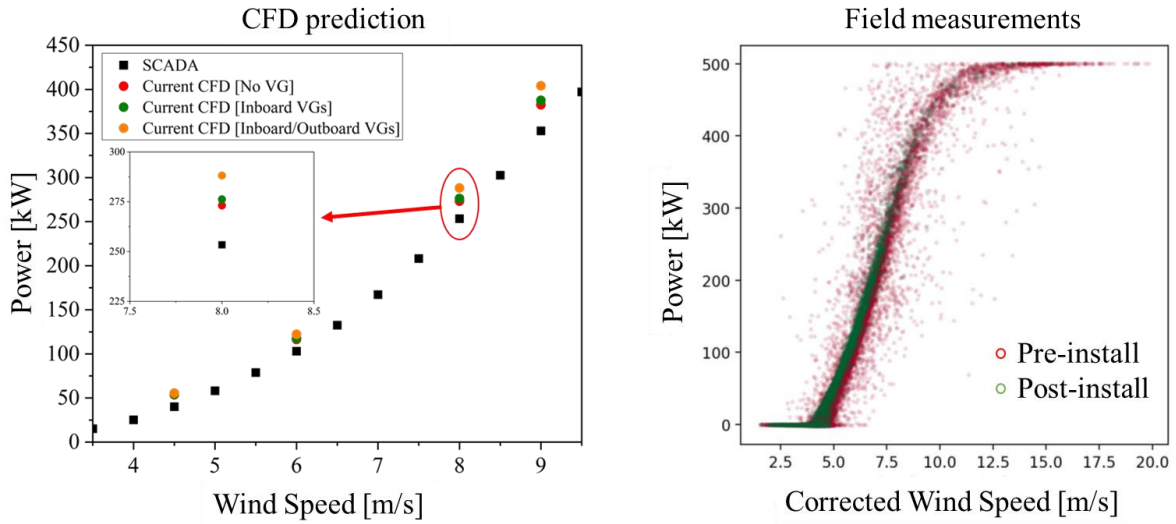

Figure 12. Power output from the V52 turbine with and without Vortex Generators. (left) CFD prediction; (right) Field measurements.

3.4. Upgrade pack performance assessment

The full retrofit upgrade pack was designed for and installed on an 850 kW Vestas V52 turbine with hub height of 40m. It is noted that the turbine is restricted to 500 kW therefore comparison with the warranted

power curve has not been performed. The pre-installation turbine performance was assessed based on 10-minute SCADA data spanning the period between 03/2021 and 03/2023. At the time of writing only one month of post-installation data have been processed. A nacelle mounted Lidar was used for wind speed velocity measurements and the Lidar data was corrected from the measurement distance (8m) to free stream velocity at 2.5 rotor diameters (100m), based on a CFD induction zone correction. The density corrected AEP uplift has been determined as 5.77%, which is consistent with the numerical analysis, which considered inboard and outboard VGs but not the gurney flap.

4. Conclusion

A comprehensive investigation was undertaken to design VGs and GFs that perform better than the current industry standard. A suite of tools was employed, including wind tunnel measurements, RANS CFD simulations, Infrared thermography, Lidar and SCADA data to design and assess the performance of an upgrade pack bespoke for a Vestas V52 turbine. The selected VG shape was a 3D twisted aerodynamically shaped VGs. The VG positioning was informed based on CFD simulations and Thermography measurements. The results show that the integrated approach was successful, achieving an AEP increase of 5.77%. A similar VG upgrade pack has been developed for a multi-MW machine and will be installed in the future.

References

[1] Hwangbo H, Ding Y, Eisele O, Weinzierl G, Lang U, Pechlivanoglou G. Quantifying the effect of vortex generator installation on wind power production: An academia-industry case study. Renew Energy 2017;113:1589–97. https://doi.org/10.1016/j.renene.2017.07.009.

[2] Chng L, Alber J, Ntouras D, Papadakis G, Kaufmann N, Ouro P, et al. On the combined use of Vortex Generators and Gurney Flaps for turbine airfoils. J Phys Conf Ser 2022;2265:032040. https://doi.org/10.1088/1742-6596/2265/3/032040.

[3] Alber J, Soto-Valle R, Manolesos M, Bartholomay S, Nayeri CN, Schönlau M, et al. Aerodynamic effects of Gurney flaps on the rotor blades of a research wind turbine. Wind Energy Sci 2020;5:1645–62. https://doi.org/10.5194/wes-5-1645-2020.

[4] Alber J, Pechlivanoglou G, Paschereit CO. Parametric Investigation of Gurney Flaps for the Use on Wind Turbine Blades. ASME Turbo Expo, Charlotte, NC: American Society of Mechanical Engineers; 2017, p. GT2017-64475.

[5] Seel F, Lutz T, Krämer E. Numerical Study of the Unsteady Blade Root Aerodynamics of a 2MW Wind Turbine Equipped With Vortex Generators. Wind Energy Sci Discuss 2023;2023:1–28.

[6] Manolesos M, Voutsinas SG. Experimental investigation of the flow past passive vortex generators on an airfoil experiencing three-dimensional separation. J Wind Eng Ind Aerodyn 2015;142:130–48. https://doi.org/10.1016/j.jweia.2015.03.020.

[7] Baldacchino D, Ferreira C, Tavernier D De, Timmer WA, van Bussel GJW. Experimental parameter study for passive vortex generators on a 30% thick airfoil. Wind Energy 2018;21:745–65. https://doi.org/10.1002/we.2191.

[8] Ravishankara AK, Bakhmet I, Özdemir H. Estimation of roughness effects on wind turbine blades with vortex generators. J. Phys. Conf. Ser., vol. 1618, IOP Publishing; 2020, p. 52031.

[9] Miller GE. Comparative performance tests on the Mod-2, 2.5-MW wind turbine with and without vortex generators. DASCON Eng. Collect. Pap. Wind Turbine Technol., 1995.

[10] Baldacchino D, Manolesos M, Ferreira C, González Salcedo Á, Aparicio M, Chaviaropoulos T, et al. Experimental benchmark and code validation for airfoils equipped with passive vortex generators. J Phys Conf Ser 2016;753:022002. https://doi.org/10.1088/1742-6596/753/2/022002.

[11] Manolesos M, Sørensen NN, Troldborg N, Florentie L, Papadakis G, Voutsinas S. Computing the flow past Vortex Generators: Comparison between RANS Simulations and Experiments. J Phys Conf Ser 2016;753:022014. https://doi.org/10.1088/1742-6596/753/2/022014.

[12] Ntouras D, Manolas D, Papadakis G, Riziotis V. Exploiting the limit of BEM solvers in moonpool type floaters. J. Phys. Conf. Ser., vol. 1618, IOP Publishing; 2020, p. 52059.
[13] Lin JC. Review of research on low-profile vortex generators to control boundary-layer separation. Prog Aerosp Sci 2002;38:389–420. https://doi.org/10.1016/s0376-0421(02)00010-6.
[14] Wendt BJ. Parametric study of vortices shed from airfoil vortex generators. AIAA J 2004;42:2185–95. https://doi.org/10.2514/1.3672.
[15] Soto-Valle R, Bartholomay S, Nayeri CN, Paschereit CO, Manolesos M. Airfoil Shaped Vortex Generators applied on a Research Wind Turbine. AIAA Scitech 2021 Forum, Reston, Virginia: American Institute of Aeronautics and Astronautics; 2021, p. 1413. https://doi.org/10.2514/6.2021-1413.
[16] Hansen MOL, Velte CM, Øye S, Hansen R, Sørensen NN, Madsen J, et al. Aerodynamically shaped vortex generators. Wind Energy 2016;19:563–7.
[17] Tian Q, Corson D, Baker J. Application of vortex generators to wind turbine blades. 34th Wind Energy Symp 2016:1–14. https://doi.org/10.2514/6.2016-0518.
[18] Zhao Z, Li T, Wang T, Liu X, Zheng Y. Numerical investigation on wind turbine vortex generators employing transition models. J Renew Sustain Energy 2015;7. https://doi.org/10.1063/1.4938122.
[19] Mueller-Vahl H, Pechlivanoglou G, Nayeri CN, Paschereit CO. Vortex generators for wind turbine blades: A combined wind tunnel and wind turbine parametric study. ASME Turbo Expo 2012.
[20] Wu Z, Chen T, Wang H, Shi H, Li M. Investigate aerodynamic performance of wind turbine blades with vortex generators at the transition area. Wind Eng 2022;46:615–29. https://doi.org/10.1177/0309524X211038542.
[21] Alber J, Manolesos M, Weinzierl G, Schönmeier A, Nayeri CN, Paschereit CO, et al. Experimental investigation of Mini-Gurney Flaps in combination with vortex generators for aerodynamic improvements of wind turbine blades. Wind Energy Sci. Conf. - EAWE, Hannover, Germany: EAWE; 2021.
[22] Papadakis G, Voutsinas SG. In view of accelerating CFD simulations through coupling with vortex particle approximations. J Phys Conf Ser 2014;524:12126. https://doi.org/10.1088/1742-6596/524/1/012126.
[23] Jirasek A. Vortex-Generator Model and Its Application to Flow Control. J Aircr 2005;42:1486–91. https://doi.org/10.2514/1.12220.
[24] Manolesos M, Papadakis G, Voutsinas SGG. Revisiting the assumptions and implementation details of the BAY model for vortex generator flows. Renew Energy 2020;146:1249–61. https://doi.org/10.1016/j.renene.2019.07.063.
[25] Manolesos M, Papadakis G, Voutsinas SG. Assessment of the CFD capabilities to predict aerodynamic flows in presence of VG arrays. J Phys Conf Ser 2014;524:012029. https://doi.org/10.1088/1742-6596/524/1/012029.
[26] Manolesos M, Chng L, Kaufmann N, Ouro P, Ntouras D, Papadakis G. Using vortex generators for flow separation control on tidal turbine profiles and blades. Renew Energy 2023;205:1025–39. https://doi.org/10.1016/J.RENENE.2023.02.009.
[27] Sørensen NN, Méndez B, Muñoz A, Sieros G, Jost E, Lutz T, et al. CFD code comparison for 2D airfoil flows. J. Phys. Conf. Ser., vol. 753, Institute of Physics Publishing; 2016. https://doi.org/10.1088/1742-6596/753/8/082019.
[28] Astolfi D, Byrne R, Castellani F. Estimation of the performance aging of the vestas v52 wind turbine through comparative test case analysis. Energies 2021;14:915.